# Small delay approximation of stochastic delay differential equations

Steve Guillouzic, Ivan L'Heureux, and André Longtin

*Ottawa-Carleton Institute for Physics, University of Ottawa, Ottawa, Ontario, Canada K1N 6N5*

(Received 19 October 1998)

Delay differential equations evolve in an infinite-dimensional phase space. In this paper, we consider the effect of external fluctuations (noise) on delay differential equations involving one variable, thus leading to univariate stochastic delay differential equations (SDDE's). For small delays, a univariate nondelayed stochastic differential equation approximating such a SDDE is presented. Another approximation, complementary to the first, is also obtained using an average of the SDDE's drift term over the delayed dynamical variable, which defines a conditional average drift. This second approximation is characterized by the fact that the diffusion term is identical to that of the original SDDE. For small delays, our approach yields a steady-state probability density and a conditional average drift which are in close agreement with numerical simulations of the original SDDE. We illustrate this scheme with the delayed linear Langevin equation and a stochastic version of the delayed logistic equation. The technique can be used with any type of noise, and is easily generalized to multiple delays. [S1063-651X(99)08304-X]

PACS number(s): 02.50.Ey, 02.30.Ks, 05.40.−a

## I. INTRODUCTION

In recent decades, delay differential equations (DDE's) have become a powerful tool for the modelization of spatially distributed systems. In these systems, the geometry is often such that one can replace a propagated effect by a time delayed version of this effect. Thus an ordinary DDE may be used instead of a nondelayed partial differential equation. This is justified when the delay of interest is commensurate with, or much larger than, other time scales in the system. Deterministic DDE's can generate several different types of asymptotic dynamics, such as fixed points, limit cycles, and chaos. They can also exhibit multistability. These behaviors have allowed DDE's to be useful in several fields. For example, DDE's have been used to model optical devices [1–4], population dynamics [5], physiological systems [6–8], neural networks [9], economic phenomena [10], and chemical kinetics [11].

When modeling systems which do not noticeably affect their environment, stochastic variables are often used to model the environmental fluctuations, thus leading to stochastic delay differential equations (SDDE's). Models stated in terms of SDDE's have already started to appear in several fields, such as physiology [7,12–14] and optics [15,16].

Stochastic terms have been shown to have a profound impact on systems described by nondelayed differential equations, leading even to qualitative modifications of a system's behavior [17,18]. The same is expected for SDDE's, and can indeed be verified numerically [12,19]. However, analytical tools for SDDE's are scarce since the ones used to study nondelayed stochastic differential equations (SDE's) [17,18] cannot, in general, be directly applied to SDDE's. Some work has been done relative to the exponential stability of SDDE's [20] and to the existence of smooth probability densities [21]. However, there is in general no way to evaluate the probability densities associated with SDDE's.

A noteworthy exception is the delayed linear Langevin equation (see Sec. IV A). Indeed, when additive white noise is considered, its linearity allows the exact determination of its sample paths and of its stationary statistical properties [22]. This linearity has also been used to study the stability of the first two moments of the steady-state probability density when subjected to additive/multiplicative white/colored noise [23]. Also, a correspondence has been established between the delayed linear Langevin equation and a delayed random walk, and this has been used to derive an approximate Fokker-Planck equation, thus leading to an approximate expression for the steady-state probability density [24,25].

Unfortunately, the tools which rely on the linearity of the SDDE cannot be used for nonlinear SDDE's. Coupled map lattices have been suggested as an alternative approach for the study of both deterministic and stochastic delay differential equations [26]. Such maps can be set to an arbitrary precision by adjusting the number of variables. This approach is particularly suited when the evolution of the probability density is sought through numerical simulations. However, the high number of variables involved in such systems has hindered analytical progress. In general, this problem cannot be avoided since a SDDE is basically a functional differential equation, and thus effectively contains an infinite number of degrees of freedom.

In certain regimes, however, the degrees of freedom may be slaved to one another. It may therefore be possible to consider only a limited number of special degrees of freedom. This paper presents an approximation scheme which leads, for small delays, from a univariate SDDE to an approximate univariate nondelayed SDE. From it, a Fokker-Planck equation and the steady-state probability density are then obtained using standard techniques [17,18]. The steady-state probability density is then used to obtain a second approximate nondelayed SDE. The importance of this approach lies in its versatility: it can be used for a large class of SDDE's.

Section II lays the foundations for the small delay approximation. It shows why the usual Fokker-Planck equation approach cannot be applied directly to a SDDE, introduces the concept of conditional average drift, and indicates how the steady-state conditional average drift can be calculated

once the steady-state probability density is known. The small delay approximation scheme, presented in Sec. III, starts with a Taylor expansion to quadratic order in the delay, and proceeds through the calculation of the steady-state probability density and conditional average drift. The latter then yields another valid approximation. This scheme is applied to two sample systems in Sec. IV. The first one is the delayed linear Langevin equation, which can be considered as a reference point since its steady-state probability density is already known, albeit not through a Fokker-Planck approach. The second system to be considered is the delayed logistic equation [27]. This is a generalization of the well-known logistic equation, which was one of the first models used in population dynamics. For each system, numerical simulations are compared to analytical predictions. Finally, Sec. V discusses the results and indicates future paths of research. An appendix completes the paper.

## II. FOKKER-PLANCK EQUATION

The systems considered in this paper are described by a state variable $x$, confined to $[a,b]$, which evolves according to the stochastic delay differential equation

$$dx(t) = f(x(t), x(t-\tau))dt + \sigma g(x(t))dW(t), \quad (1)$$

where $f(x_o, x_\tau)$ and $g(x_o)$ are known functions, $\tau$ is the delay, and $\sigma$ is a parameter which scales the noise amplitude. Throughout this paper, $x_o$ and $x_\tau$ are used as dummy variables, and do not necessarily refer to $x(t)$ and $x(t-\tau)$, nor to initial conditions. The quantity $W(t)$ in Eq. (1) is a Wiener process whose initial condition is 0 at time $t=0$. It is hence characterized by

$$\langle W(t) \rangle = 0$$

and

$$\langle W^2(t) \rangle = t,$$

where $\langle \cdots \rangle$ denotes an ensemble average (average over realizations).

Up to Sec. III, Eq. (1) is interpreted using Ito calculus. In order to study a Stratonovich differential equation in Sec. IV B, we first transform it into an equivalent Ito differential equation, after which the formalism developed here for the latter can be applied. This is discussed in the Appendix.

Let $G(x_o)$ be an arbitrary $C^2$ function defined on $[a,b]$, and for which

$$\lim_{x_o \to a} G(x_o) = \lim_{x_o \to b} G(x_o) = 0 \quad (2a)$$

and

$$\lim_{x_o \to a} \frac{d}{dx_o} G(x_o) = \lim_{x_o \to b} \frac{d}{dx_o} G(x_o) = 0. \quad (2b)$$

Then

$$dG(x(t)) = G(x(t) + dx(t)) - G(x(t)). \quad (3)$$

If $G(x(t) + dx(t))$ is developed in a Taylor series around $x(t)$, using Eq. (1), and only terms up to first order in $dt$ are kept, Eq. (3) becomes

$$dG(x(t)) = \left\{ f(x(t), x(t-\tau)) \frac{d}{dx_o} G(x(t)) \right.$$
$$+ \frac{\sigma^2}{2} g^2(x(t)) \frac{d^2}{dx_o^2} G(x(t)) \right\} dt$$
$$\left. + \sigma g(x(t)) \frac{d}{dx_o} G(x(t)) dW(t), \quad (4)$$

where $(dW(t))^2 = dt$ has been used, as well as the definition

$$\frac{d}{dx_o} G(x(t)) \equiv \frac{d}{dx_o} G(x_o) \bigg|_{x_o = x(t)}.$$

Equation (4) is the well-known Ito formula, but derived for a SDDE. It has the same form as for a nondelayed SDE [17]. The ensemble average of $dG(x(t))$ can be written as

$$\left\langle \frac{d}{dt} G(x(t)) \right\rangle = \left\langle f(x(t), x(t-\tau)) \frac{d}{dx_o} G(x(t)) + \frac{\sigma^2}{2} g^2(x(t)) \frac{d^2}{dx_o^2} G(x(t)) \right\rangle, \quad (5)$$

since $dW(t)$ is independent of $x(t)$ and $x(t-\tau)$, and since $\langle dW(t) \rangle = 0$. In order to evaluate these averages, an appropriate probability density must be defined. Let $p(x_o, t_o; x_\tau, t_\tau | \phi) dx_o dx_\tau$ be the probability that $x(t_o) \in [x_o, x_o + dx_o]$ and $x(t_\tau) \in [x_\tau, x_\tau + dx_\tau]$, given that $x(t) = \phi(t)$ for all $t \in [-\tau, 0]$. Thus $p(x_o, t_o; x_\tau, t_\tau | \phi)$ is a bivariate probability density which is conditional only on the initial condition $\{\phi(t) | t \in [-\tau, 0]\}$. The averages in Eq. (5) can then be expressed in terms of this probability density, leading to

$$\int_a^b dx_o G(x_o) \int_a^b dx_\tau \frac{\partial}{\partial t} p(x_o, t; x_\tau, t-\tau | \phi)$$

$$= \int_a^b dx_o G(x_o) \int_a^b dx_\tau \left\{ -\frac{\partial}{\partial x_o} [f(x_o, x_\tau) p(x_o, t; x_\tau, t-\tau | \phi)] + \frac{\sigma^2}{2} \frac{\partial^2}{\partial x_o^2} [g^2(x_o) p(x_o, t; x_\tau, t-\tau | \phi)] \right\},$$

where the right-hand side has been integrated by parts with respect to $x_o$ and surface terms have been neglected as a consequence of Eqs. (2a) and (2b). Since $G(x_o)$ is arbitrary, this equation leads to

$$\frac{\partial}{\partial t}p(x_o,t|\phi)=-\frac{\partial}{\partial x_o}\left\{p(x_o,t|\phi)\int_a^b dx_\tau f(x_o,x_\tau)p(x_\tau,t-\tau|x_o,t;\phi)\right\}+\frac{\sigma^2}{2}\frac{\partial^2}{\partial x_o^2}\{p(x_o,t|\phi)g^2(x_o)\}, \quad (6)$$

where the order in which the integral and the derivatives are performed has been reversed, and where

$$p(x_o,t_o|\phi)\equiv\int_a^b dx_\tau p(x_o,t_o;x_\tau,t_\tau|\phi) \quad (7)$$

and

$$p(x_\tau,t_\tau|x_o,t_o;\phi)\equiv\frac{p(x_o,t_o;x_\tau,t_\tau|\phi)}{p(x_o,t_o|\phi)}. \quad (8)$$

Thus $p(x_o,t_o|\phi)$ is a univariate probability density conditional only on the initial condition, while $p(x_\tau,t_\tau|x_o,t_o;\phi)$ is a univariate probability density conditional both on the fact that $x(t_o)=x_o$ and on the initial condition. Let

$$\bar{f}(x_o,t_o|\phi)\equiv\int_a^b dx_\tau f(x_o,x_\tau)p(x_\tau,t_o-\tau|x_o,t_o;\phi), \quad (9)$$

which is called the conditional average drift (CAD). Since $\langle W(t)\rangle=0$, the CAD is seen to be the average of $(d/dt)x(t)$ at time $t_o$ given that $x(t_o)=x_o$, thus its name. Using this CAD, Eq. (6) becomes

$$\frac{\partial}{\partial t}p(x_o,t|\phi)=-\frac{\partial}{\partial x_o}\{\bar{f}(x_o,t|\phi)p(x_o,t|\phi)\}$$
$$+\frac{\sigma^2}{2}\frac{\partial^2}{\partial x_o^2}\{g^2(x_o)p(x_o,t|\phi)\}, \quad (10)$$

which is the well-known Fokker-Planck equation (FPE). As is easily seen, the SDE

$$dx(t)=\bar{f}(x(t),t|\phi)dt+\sigma g(x(t))dW(t), \quad (11)$$

in which the diffusion term is the same as in Eq. (1), would lead to the same FPE [Eq. (10)].

Assuming that the system approaches a steady-state limit as $t\to\infty$, the functions $\bar{f}^s(x_o|\phi)$ and $p^s(x_o|\phi)$ are defined as being, respectively, the steady-state limits of $\bar{f}(x_o,t|\phi)$ and $p(x_o,t|\phi)$. If the boundaries are reflecting, Eq. (10) then leads to the so-called potential solution

$$p^s(x_o|\phi)=\frac{N}{g^2(x_o)}\exp\left(\frac{2}{\sigma^2}\int_c^{x_o}dx'\frac{\bar{f}^s(x'|\phi)}{g^2(x')}\right), \quad (12)$$

where $c\in[a,b]$. The constant $N$ is determined from the normalization condition

$$\int_a^b dx_o p^s(x_o|\phi)=1,$$

and implicitly depends on $\tau$.

As the delay vanishes,

$$\lim_{\tau\to0}p(x_o,t_o|x_\tau,t_o-\tau;\phi)=\delta(x_o-x_\tau),$$

leading to

$$\bar{f}(x_o,t_o|\phi)=f(x_o,x_o).$$

Thus Eq. (10) approaches the usual FPE associated with a SDE.

Though Eq. (10) is a formally exact Fokker-Planck equation for the SDDE given by Eq. (1), and though Eq. (12) is the corresponding steady-state probability density, these equations are somewhat problematic since they are not self-sufficient. Indeed, the CAD $\bar{f}(x_o,t_o|\phi)$ must first be evaluated, and this may not be an easy task. Despite this fact, these equations constitute an invaluable tool as a starting point for approximation schemes or when used in conjunction with them. In particular, Sec. III presents an approximation scheme which allows the determination of $p^s(x_o|\phi)$ in the small delay regime. Once Eq. (12) is inverted to yield

$$\bar{f}^s(x_o|\phi)=\frac{\sigma^2}{2}g^2(x_o)\frac{d}{dx_o}\ln p^s(x_o|\phi)+\sigma^2 g(x_o)\frac{d}{dx_o}g(x_o), \quad (13)$$

the steady-state CAD $\bar{f}^s(x_o|\phi)$ can also be evaluated. As discussed in Secs. III and IV, the steady-state CAD leads to another valid approximate SDE.

## III. SDDE EXPANSION TO $O(\tau^2)$

For small delays, $f(x(t),x(t-\tau))$ can be expanded in powers of $\tau$ using a Taylor expansion around $x(t)$. Indeed, such an expansion has been shown to be valid to quadratic order in $\tau$ [28]. It leads from the SDDE (1) to

$$dx=f_a(x)dt+\sigma g_a(x)dW, \quad (14)$$

where

$$f_a(x_o)\equiv f(x_o,x_o)\left(1-\tau\frac{\partial}{\partial x_\tau}f(x_o,x_o)\right), \quad (15a)$$

$$g_a(x_o)\equiv g(x_o)\left(1-\tau\frac{\partial}{\partial x_\tau}f(x_o,x_o)\right), \quad (15b)$$

and

$$\frac{\partial}{\partial x_\tau}f(x_o,x_o)\equiv\frac{\partial}{\partial x_\tau}f(x_o,x_\tau)\bigg|_{x_\tau=x_o}.$$

In these equations, the subscript $a$ stands for "approximate," and time is dropped since it is the same for all variables. Equation (14) constitutes an approximate SDE which approaches the exact SDDE as the delay vanishes.

Let $p_a(x_o,t_o|\phi_o)dx_o$ be the probability that $x(t_o)$ $\in[x_o,x_o+dx_o]$ given that $x(0)=\phi_o\equiv\phi(0)$ for a system whose evolution is given by Eq. (14). Then, following a procedure [17,18] similar to what is done in Sec. II, the FPE corresponding to this equation is found to be

$$\frac{\partial}{\partial t}p_a(x_o,t|\phi_o)=-\frac{\partial}{\partial x_o}\{f_a(x_o)p_a(x_o,t|\phi_o)\}$$
$$+\frac{\sigma^2}{2}\frac{\partial^2}{\partial x_o^2}\{g_a^2(x_o)p_a(x_o,t|\phi_o)\},\quad(16)$$

and the steady-state probability density is

$$p_a^s(x_o|\phi_o)=\frac{N_a}{g_a^2(x_o)}\exp\left(\frac{2}{\sigma^2}\int_c^{x_o}dx'\frac{f_a(x')}{g_a^2(x')}\right),\quad(17)$$

where $N_a$ is the normalization constant and $c$ is within the support. This support need not be $[a,b]$, since it may have been slightly modified by the expansion. As in Eq. (12), the normalization constant implicitly depends on $\tau$. Also, even though the initial condition $\phi_o$ does not appear on the right-hand side of Eq. (17), it may still affect the probability density through its possible influence on the support.

Finally, using Eq. (13) with Eq. (17) allows the determination of the approximate steady-state CAD

$$\bar{f}^s(x_o|\phi)=\frac{f(x_o,x_o)+\tau\sigma^2g^2(x_o)\left[\frac{d}{dy}\frac{\partial}{\partial x_\tau}f(y,y)\right]_{y=x_o}}{1-\tau\frac{\partial}{\partial x_\tau}f(x_o,x_o)},$$
$$(18)$$

where, as before,

$$\frac{\partial}{\partial x_\tau}f(y,y)\equiv\frac{\partial}{\partial x_\tau}f(x_o,x_\tau)\bigg|_{x_o=y,\ x_\tau=y}.$$

Equation (18) is an approximate expression for the steady-state CAD of the SDDE, which is the steady-state average of $f(x_o,x_\tau)$ over $x_\tau$. The situation is much simpler when considering a nondelayed SDE. Since the drift term does not involve any delayed $x$'s, the CAD is the drift term itself. For example, in Eq. (14), the CAD is $f_a(x_o)$.

It is interesting to note that the steady-state CAD $\bar{f}^s(x_o|\phi)$ is not equal to $f_a(x_o)$, the drift term of the approximate system arising from the Taylor expansion. This difference is due to the fact that the delay modifies both the drift and the diffusion terms in the approximate system of Eq. (14), whereas it does not appear in the diffusion term of the exact system. Therefore, the CAD must integrate the modifications which are incurred by both the drift and the diffusion terms in the approximate SDE based on $f_a(x_o)$ and $g_a(x_o)$. The examples presented in Sec. IV clearly illustrate the difference between the two drifts and the benefit of using the CAD.

The steady-state CAD given by Eq. (18), in conjunction with Eq. (11), leads to the approximate SDE

$$dx=\bar{f}^s(x|\phi)dt+\sigma g(x)dW,\quad(19)$$

where $g(x_o)$ is the same as in the original SDDE (1). The steady-state CAD $\bar{f}^s(x_o|\phi)$ is calculated in such a way that Eq. (19) has the same steady-state probability density as the approximate SDE based on $f_a(x_o)$ and $g_a(x_o)$. However, the two approximate SDE's obviously have different CAD's since their drift terms are different. These CAD's will both be compared with numerical simulation results in Sec. IV.

Clearly, Eqs. (17) and (18) have not been completely expanded to quadratic order in $\tau$, since the delay appears nonlinearly in them. This is due to the fact that no term has been dropped after the transition from SDDE (1) to SDE (14). Within the range of $x$'s over which Eqs. (17) and (18) are quantitatively accurate, systematic quadratic order expansions in $\tau$ of these equations ought to be as accurate as the originals. Outside this range however, the probability density and the conditional average drift may undergo qualitative modifications when subjected to complete quadratic order expansions. In particular, their convergence radii may be altered. Since Eqs. (17) and (18) follow directly from a SDE which, for small delays, is close to the original SDDE, they have a better chance of exhibiting an overall qualitatively accurate behavior than systematic quadratic order expansions. The delayed logistic case presented in Sec. IV B is a good example of this. It therefore seems appropriate that systematic quadratic order expansions be carried out only on a case by case basis and not in the general theory.

Finally, as the delay goes to zero, $f_a(x_o)\rightarrow f(x_o,x_o)$ and $g_a(x_o)\rightarrow g(x_o)$. The steady-state probability density $p_a^s(x_o|\phi_o)$ and the CAD $\bar{f}^s(x_o|\phi)$ thus tend to the corresponding quantities of the nondelayed SDE obtained by setting $\tau=0$ in Eq. (1).

## IV. APPLICATIONS

### A. Delayed linear Langevin equation

#### 1. Deterministic equation

The linear delay differential equation

$$\frac{d}{dt}x(t)=-\alpha x(t-\tau),\quad(20)$$

where $\alpha$ is a positive coefficient, was studied by Wright [29]. In particular, its eigenvalues, around its one and only fixed point $x(t)=0$, can be determined by substituting in it the sample function $x(t)=Ae^{\lambda t}$, where $\lambda$ is complex. This leads to the characteristic equation

$$\lambda=-\alpha e^{-\lambda\tau}.$$

Figure 1 summarizes the behavior of the roots. For $\tau=0$, this equation has only one root: $\lambda=-\alpha$. As $\tau$ increases from 0, this root becomes more negative, and an infinite number of roots arise whose real parts increase from $-\infty$. One of these new roots is real; the others are complex conjugate pairs. The complex roots emerge with imaginary parts which are, in absolute value, arbitrarily large for arbitrarily small $\tau$. As the delay increases, they grow closer to the imaginary axis as well as to the real axis. At $\tau=1/\alpha e$, the new real root merges

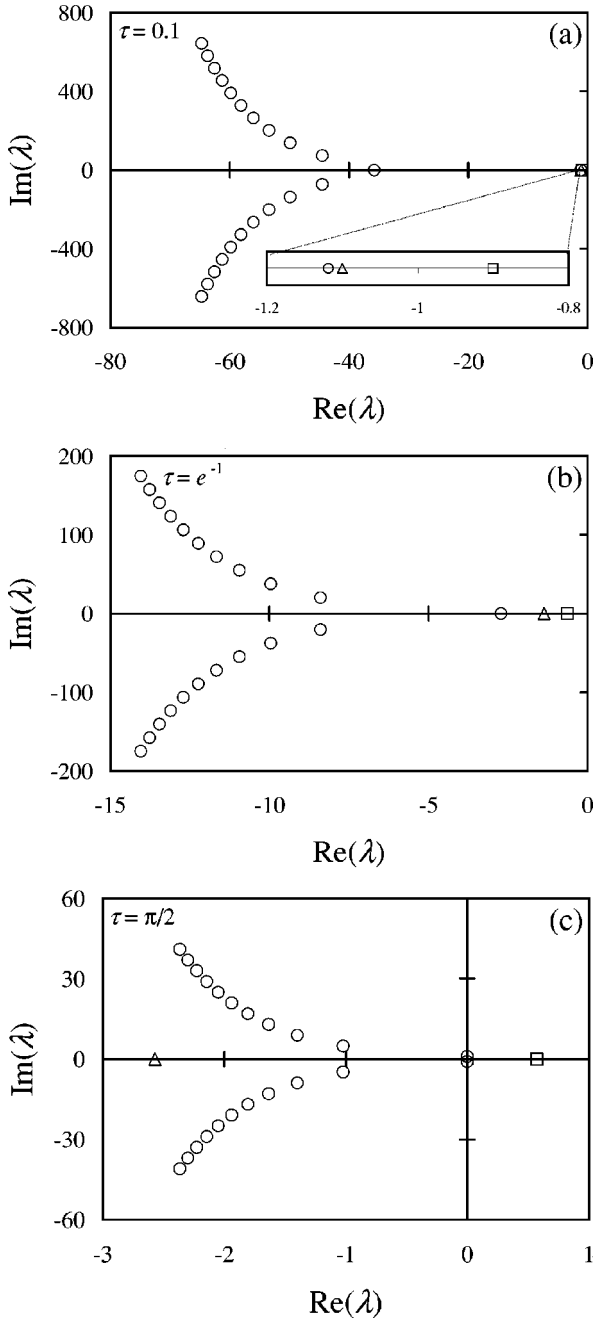FIG. 1. Eigenvalues of the linear deterministic DDE (20) and of the determininstic part of the two approximate SDE's (30) and (34) for $\alpha = 1$ and various values of the delay. The circles represent, for Eq. (20), the 11 pairs of eigenvalues with the least negative real parts. The triangle represents the eigenvalue of the deterministic part of the approximate SDE based on $f_a(x_o)$ and $g_a(x_o)$ [Eq. (30)], and the square the same based on $\bar{f}^s(x_o|\phi)$ [Eq. (34)]. On graph (a), three eigenvalues are so close that an enlargement is required. On graph (b), the two real eigenvalues of Eq. (20) are merging. On graph (c), a pair of eigenvalues of Eq. (20) is located on the $y$ axis, near the origin.

with the old one, and they become a complex conjugate pair whose real part increases with the delay. At $\tau = \pi/2\alpha$, this pair crosses the imaginary axis. For $\tau > \pi/2\alpha$, their real part is therefore positive.

Consequently, at $\tau = 0$ the system decays monotonically since the only eigenvalue is real and negative. For $0 < \tau$ $<1/\alpha e$, the system also decays monotonically for constant initial conditions, since all the eigenvalues have negative real parts. Finally for $1/\alpha e < \tau < \pi/2\alpha$, the system undergoes damped oscillations, and for $\tau > \pi/2\alpha$ diverging oscillations.

### 2. Exact expression for the variance

Before applying the results of Sec. III to this problem, an exact expression for the variance of the state variable is derived below using the linear properties of the SDDE. This expression is then used as a reference point for the approximate expression calculated in Sec. IV A 3.

*(a) Wide-sense stationary noise.* Adding the noise term $\eta(t)$ to Eq. (20) leads to the SDDE

$$\frac{d}{dt}x(t) = -\alpha x(t-\tau) + \eta(t), \quad (21)$$

where $\eta(t)$ is a given wide-sense stationary (WSS) stochastic process, i.e., a process for which $\langle \eta(t) \rangle$ is constant and for which $\langle \eta(t_1) \eta(t_2) \rangle$ depends only on $t_2 - t_1$ [30]. Once $x(t)$'s initial condition has decayed, Eq. (21) is a linear time-invariant transformation. Therefore, $x(t)$ is also a WSS stochastic process. Furthermore, in this stationary regime, $x(t)$ and $\eta(t)$ are jointly WSS, i.e., $x(t)$ and $\eta(t)$ are WSS and $\langle x(t_1) \eta(t_2) \rangle$ depends only on $t_2 - t_1$ [30].

Taking the average of Eq. (21) allows the determination of an evolution equation for the ensemble average of $x(t)$. Indeed,

$$\frac{d}{dt}\langle x(t) \rangle = -\alpha \langle x(t-\tau) \rangle, \quad (22)$$

where $\langle \eta(t) \rangle$ has been set to zero with no loss of generality since it is constant for a WSS stochastic process. The stability analysis carried out for Eq. (20) also applies to this one. In particular, $\langle x(t) \rangle = 0$ is the only fixed point.

Since $x(t)$ and $\eta(t)$ are jointly WSS, the correlation functions $R_{xx}(\Delta t) \equiv \langle x(t) x(t+\Delta t) \rangle$, $R_{x\eta}(\Delta t) \equiv \langle x(t) \eta(t+\Delta t) \rangle$, and $R_{\eta\eta}(\Delta t) \equiv \langle \eta(t) \eta(t+\Delta t) \rangle$ do not depend on $t$. Using Eq. (21) leads to

$$\frac{d}{dt}R_{x\eta}(t) = -\alpha R_{x\eta}(t-\tau) + R_{\eta\eta}(t) \quad (23a)$$

and

$$\frac{d}{dt}R_{xx}(t) = \alpha R_{xx}(t+\tau) - R_{x\eta}(t), \quad (23b)$$

where $t \equiv t_2 - t_1$.

Let the Fourier transform of a function $R(t)$ be defined as

$$S(\omega) \equiv \mathcal{F}\{R(t)\} \equiv \int_{-\infty}^{\infty} dt\, e^{i\omega t} R(t).$$

Then, taking the Fourier transform of Eqs. (23a) and (23b), and introducing the spectral densities $S_{xx}(\omega) \equiv \mathcal{F}\{R_{xx}(t)\}$ and $S_{\eta\eta}(\omega) \equiv \mathcal{F}\{R_{\eta\eta}(t)\}$, leads to

$$S_{xx}(\omega) = \frac{S_{\eta\eta}(\omega)}{\alpha^2 + \omega^2 - 2\alpha\omega \sin(\omega\tau)}. \quad (24)$$

Using a slightly different approach, a compatible expression for the spectrum of a damped delayed linear Langevin equation was obtained by Hunter and Milton [31].

Since $\langle x(t) \rangle = 0$ in the stationary regime, the variance $\sigma_x^2$ of $x(t)$ is given by

$$\sigma_x^2 = R_{xx}(0) = \frac{1}{2\pi} \int_{-\infty}^{\infty} d\omega \frac{S_{\eta\eta}(\omega)}{\alpha^2 + \omega^2 - 2\alpha\omega \sin(\omega\tau)} . \tag{25}$$

*(b) Gaussian white noise.* If $\eta(t)$ is set to Gaussian white noise, i.e., $\eta(t)dt = \sigma dW(t)$, Eq. (21) becomes

$$dx(t) = -\alpha x(t-\tau)dt + \sigma dW(t). \tag{26}$$

The noise spectrum is then given by $S_{\eta\eta} = \sigma^2$, and the variance of $x(t)$, by

$$\sigma_x^2 = \frac{\sigma^2}{2\pi} \int_{-\infty}^{\infty} d\omega \frac{1}{\alpha^2 + \omega^2 - 2\alpha\omega \sin(\omega\tau)} . \tag{27}$$

Furthermore, since $x(t)$ and $\eta(t)$ are jointly WSS, $x(t)$ is also Gaussian. This means that its probability density is fully determined by its average and variance.

When numerically integrated, Eq. (27) is seen to be equivalent, for a delay between 0 and $\pi/2\alpha$, to a special case of a closed form expression obtained by Küchler and Mensch [22] for a damped delayed linear Langevin equation subjected to white noise. When specialized to the problem considered here, their expression can be written as

$$\sigma_x^2 = \frac{\sigma^2}{2\alpha} \left[ \frac{1 + \sin(\alpha\tau)}{\cos(\alpha\tau)} \right], \tag{28}$$

using our notation.

A Taylor expansion of Eq. (27), or Eq. (28), in powers of $\tau$ around $\tau = 0$ leads, to quadratic order in $\tau$, to

$$\sigma_x^2 = \frac{\sigma^2}{2\alpha} (1 + \alpha\tau). \tag{29}$$

When this equation is considered together with the behavior of the deterministic eigenvalues as discussed in Sec. IV A 1 and illustrated in Fig. 1, there seems to be a paradox. Indeed, the deterministic eigenvalue of the delayed linear Langevin equation with the least negative real part initially drifts towards more negative values as the delay increases from zero. Intuitively, this should lead to a decreasing variance for the steady-state probability density. This is not so. In fact, the variance increases with the delay. This paradox stems from the indirect influence that the diffusion term of a SDDE has on the drift term through $x(t-\tau)$. Even though the delay does not explicitly appear in the diffusion term, it effectively modifies the influence of the noise on the system, as is shown by the presence of $\tau$ in $g_a(x_o)$ [Eq. (15b)]. For the linear SDDE, as shown in Sec. IV A 3, $g_a(x_o)$ increases with the delay, thus indicating that the SDDE becomes effectively more sensitive to noise as the delay increases.

### 3. SDDE expansion to $O(\tau^2)$

When the theory presented in Sec. III is applied to the delayed linear Langevin equation with additive Gaussian white noise [Eq. 26], it leads to the functions $f_a(x_o) = -\alpha(1+\alpha\tau)x_o$ and $g_a(x_o) = 1+\alpha\tau$, and to the approximate SDE

$$dx = -\alpha(1+\alpha\tau)x\, dt + (1+\alpha\tau)\sigma\, dW. \tag{30}$$

The corresponding approximate steady-state probability density is given by

$$p_a^s(x_o|\phi_o) = N_a \exp\left( \frac{-\alpha x_o^2}{\sigma^2(1+\alpha\tau)} \right), \tag{31}$$

where $N_a$ is the normalization constant. The variance can be directly extracted from this equation. It is thus given, to quadratic order in $\tau$, by

$$\sigma_x^2 = \frac{\sigma^2}{2\alpha}(1+\alpha\tau). \tag{32}$$

This corresponds to Eq. (29), which has been directly derived from the exact Eq. (27). Finally, using Eq. (18), the conditional average drift evaluates to

$$\bar{f}^s(x_o|\phi) = -\alpha(1-\alpha\tau)x_o \tag{33}$$

to quadratic order in $\tau$. As seen from Eqs. (31) and (33), the steady-state probability density and conditional average drift are effectively independent of the initial condition because the support is not disjoint.

The approximate SDE associated with the steady-state CAD [Eq. (33)] is

$$dx = -\alpha(1-\alpha\tau)x\, dt + \sigma\, dW. \tag{34}$$

The corresponding FPE agrees, to quadratic order in $\tau$, with the approximate FPE obtained by Ohira [24] using an approximate correspondance between Eq. (26) and a delayed random walk.

As stated at the end of Sec. III, it is normal for the two drifts $f_a(x_o)$ and $\bar{f}^s(x_o|\phi)$ to be different. Still, looking at the eigenvalues (Fig. 1) of the ordinary differential equations (ODE's) arising from these drifts in this particular system clarifies what is stated in Sec. III. The eigenvalue of the ODE $(d/dt)x = f_a(x)$ is $-\alpha(1+\alpha\tau)$, which becomes more negative as the delay increases. This is in accordance with the behavior of the original eigenvalue of Eq. (20). However, in contrast with the original SDDE, it does not seem paradoxal that the variance increases with the delay since $g_a(x_o)$ explicitly depends on $\tau$. On the other hand, the eigenvalue of the ODE $(d/dt)x = \bar{f}^s(x|\phi)$ is $-\alpha(1-\alpha\tau)$. The latter becomes less negative as the delay increases, which intuitively agrees with the fact that the variance increases with the delay, and which contrasts with what happens to the corresponding eigenvalue of Eq. (20). This is due to the fact that only the drift term, and not the diffusion term, is modified by the delay in Eq. (34). Thus the CAD must incorporate what

is incurred by $f_a(x_o)$ and $g_a(x_o)$ in Eq. (30). Overall, both Eqs. (30) and (34) are valid approximations of SDDE (26). However, as illustrated in Sec. IV A 4, Eq. (34) is the most advantageous.

### 4. Numerical simulations

Scaling $t$ by $\alpha^{-1}$ and $x$ by $\sigma$, Eqs. (26) and (30) are obtained with $\alpha = \sigma = 1$. The simulations of these two equations were performed using a fixed step size stochastic Euler integration scheme. The integration step size was varied between $10^{-3}$ and $10^{-5}$, and was never larger than one thousandth of the delay. The steady-state CAD's were obtained through a time average of one realization spanning about $10^9$ integration steps, while the steady-state probability densities used 100 realizations spanning about $10^7$ integration steps each, and the moments, 20 realizations spanning $5 \times 10^7$ integration steps each. The same numbers were used for the approximate SDE simulations. In each graph, the error bars on each point are either smaller than the symbol or of similar size.

As seen from Figs. 2 and 3, the agreement between the small delay approximation and the exact results is excellent for small delays. For example, at $\tau = 0.1$, the steady-state probability densities can hardly be distinguished from one another. Even at $\tau = 0.7$, the agreement is still reasonable. Even though there is a 20% difference in the variances, the probability densities still look quite similar. However, at $\tau = 1.2$, the quadratic order small delay approximation significantly underestimates the variance. Overall, the approximation is seen to be valid for quite a wide range of delays (up to about $\tau = 0.7$).

As stated in Sec. III, even though the SDE based on $\bar{f}^s(x_o|\phi)$ of Eq. (18) yields the same steady-state probability density as the one based on $f_a(x_o)$ and $g_a(x_o)$, they have different CAD's. Both are linear functions of $x_o$, but the slope of these linear functions behave very differently as the delay increases (Fig. 4). Clearly, $\bar{f}^s(x_o|\phi)$ is much closer to the exact SDDE's steady-state CAD than $f_a(x_o)$.

### B. Delayed logistic equation

#### 1. Deterministic equation

The next system to be considered is the delayed logistic equation [27]

$$\frac{d}{dt}x(t) = [\alpha - \beta x(t-\tau)]x(t), \tag{35}$$

where $\alpha$ and $\beta$ are positive coefficients. In the context of population dynamics, $\tau$ usually characterizes the reaction time of the population to environmental constraints, while $\beta$ scales these constraints and $\alpha$ is the Malthusian growth rate. In Eq. (35), $x(t)$ is confined to positive real numbers. Indeed, as $x(t)$ approaches zero, its time derivative also approaches zero, unless $x(t-\tau)$ simultaneously becomes arbitrarily large. It would be quite pathological for the system to diverge at a certain time and then approach zero $\tau$ units of time later. This would require a very peculiar initial condition. This being said, $x(t)$ is therefore bounded from below by the origin for any practical applications.
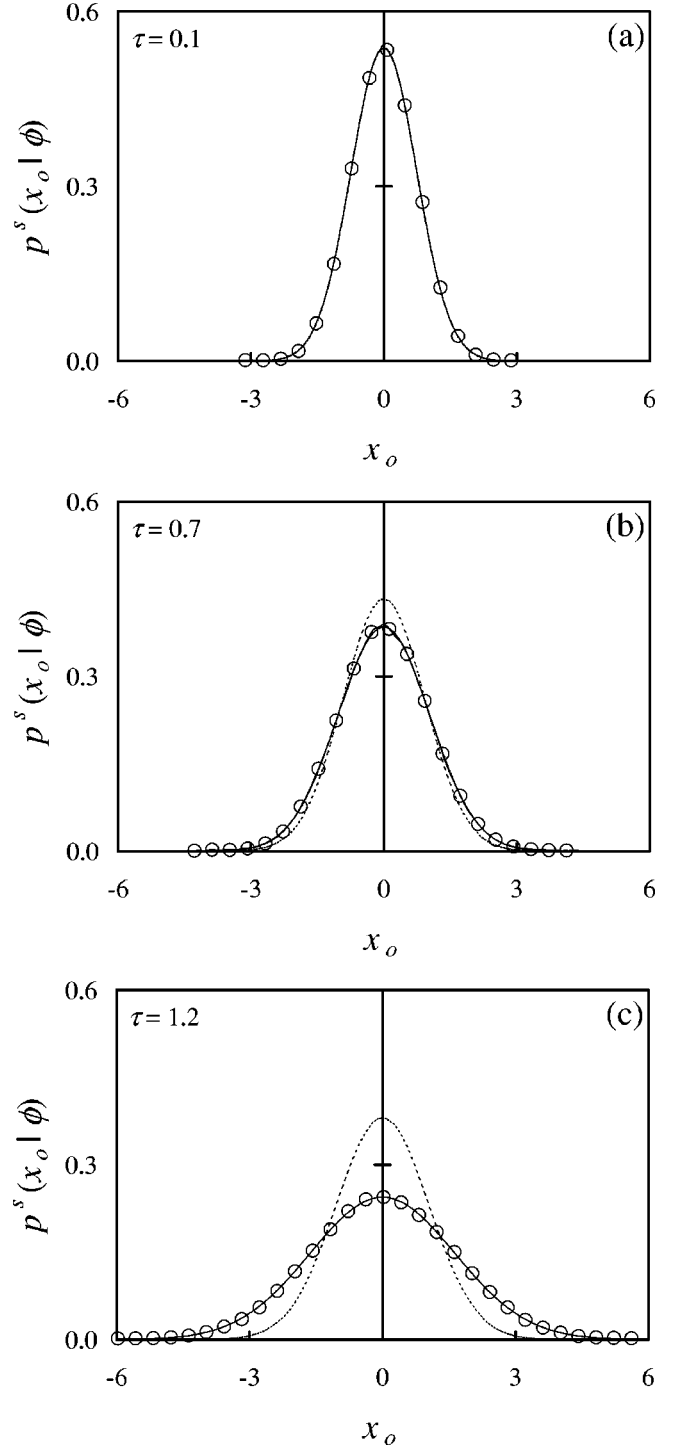


FIG. 2. Steady-state probability density of the linear SDDE (26) for various values of the delay. The circles represent simulation results. The continuous line is a Gaussian with zero mean and a variance given by Eq. (28). The dotted line is the approximate Gaussian probability density given by Eq. (31). In graph (a), the two lines are practically indistinguishable.

Equation (35) has two fixed points, $x_1 = 0$ and $x_2 = \alpha/\beta$. While $x_1$ is unstable, linearizing Eq. (35) around $x_2$ leads to Eq. (20). Thus the stability analysis performed for the delayed linear equation presented in Sec. IV A 1 can be applied to the fixed point $x_2$.
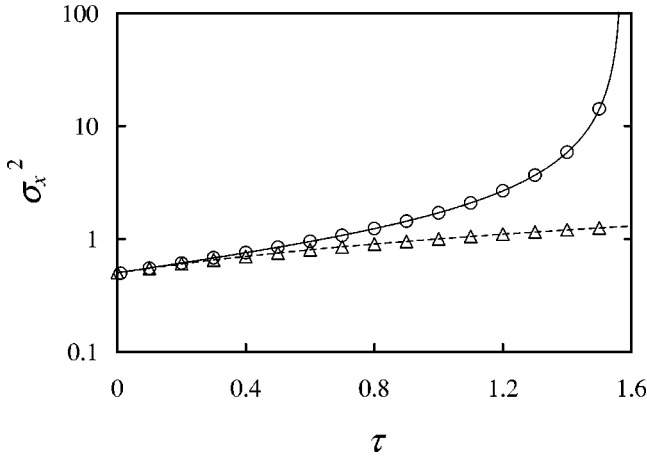
FIG. 3. Variance as a function of the delay for the linear SDDE (26) and the approximate SDE based on $f_a(x_o)$ and $g_a(x_o)$ [Eq. (30)]. The circles and triangles represent simulation results for, respectively, the linear SDDE and the approximate SDE. The continuous line is the exact expression (28) for the variance, and the dashed line the approximate expression (32). The logarithmic scale clearly shows the close agreement between the two formulas for small values of $\tau$.

### 2. SDDE expansion to $O(\tau^2)$

In this paper, we choose to make $\alpha$ a stochastic parameter in order to illustrate our approach in a multiplicative noise context. This represents fluctuations in the net relative growth rate of the population. As noise is applied to parameter $\alpha$ in Eq. (35), the latter becomes the stochastic delayed logistic equation

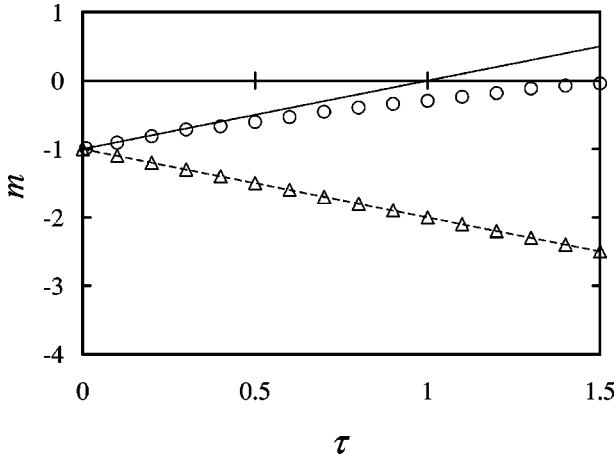$$dx(t) = [\alpha - \beta x(t-\tau)]x(t)dt + \sigma x(t)dW(t). \quad (36)$$



FIG. 4. Slope $m$ of the steady-state CAD for the linear SDDE (26) and for the approximate SDE's (30) and (34). For these equations, the steady-state CAD's are linear functions of $x_o$. This graph draws the slope $m$ of these linear relations as a function of delay. The circles represent the steady-state CAD's slope for the linear SDDE calculated using numerical simulations of the SDDE. The triangles represent the steady-state CAD's slope for the approximate SDE based on $f_a(x_o)$ and $g_a(x_o)$ [Eq. (30)], using numerical simulations of Eq. (30). The continuous line represents the slope of the steady-state CAD $\bar{f}^s(x_o|\phi)$, and the dashed line, of the drift function $f_a(x_o)$.

Since the noise term tends to zero as $x(t)$ approaches zero, the system is still bounded by the origin. Performing the Taylor expansion presented in Sec. III leads to the functions $f_a(x_o) = (1+\beta\tau x_o)(\alpha - \beta x_o)x_o$ and $g_a(x_o) = (1+\beta\tau x_o)x_o$, to the approximate SDE,

$$dx = (1+\beta\tau x)(\alpha - \beta x)x\, dt + (1+\beta\tau x)x\, dW, \quad (37)$$

and to the steady-state probability density

$$p_a^s(x_o|\phi_o) = \frac{N_a x^{2\alpha/\sigma^2 - 2}}{(1+\beta\tau x)^{2(\tau^{-1}+\alpha)/\sigma^2 + 2}}, \quad (38)$$

where $N_a$ is the normalization constant. The moments of this steady-state probability density are found to be

$$\langle x^n \rangle = \frac{\Gamma\left(\dfrac{2\alpha}{\sigma^2}+n-1\right)\Gamma\left(\dfrac{2}{\tau\sigma^2}-n+3\right)}{(\beta\tau)^n \Gamma\left(\dfrac{2\alpha}{\sigma^2}-1\right)\Gamma\left(\dfrac{2}{\tau\sigma^2}+3\right)}, \quad (39)$$

where $\Gamma(x)$ is the gamma function. In particular, the mean is given by

$$\langle x \rangle = \frac{\alpha - \sigma^2/2}{\beta(1+\tau\sigma^2)}, \quad (40)$$

and the variance by

$$\sigma_x^2 = \frac{\sigma^2\left(\alpha - \dfrac{\sigma^2}{2}\right)\left[1+\tau\left(\alpha + \dfrac{\sigma^2}{2}\right)\right]}{2\beta^2(1+\tau\sigma^2)^2\left(1+\tau\dfrac{\sigma^2}{2}\right)}. \quad (41)$$

In deriving Eq. (39), it is seen that the arguments of the gamma functions must all be non-negative. This implies that Eq. (39) can be used to calculate the moments with $n<3+2/(\tau\sigma^2)$, provided also that $\sigma^2<2\alpha$. Indeed, as seen from Eqs. (40) and (41), the mean and the variance both go to zero as $\sigma^2 \to 2\alpha$.

Finally, Eq. (18) allows the determination of an approximate expression for the steady-state CAD,

$$\bar{f}^s(x_o|\phi) = \frac{x_o}{1+\beta\tau x_o}[\alpha - \beta(1+\tau\sigma^2)x_o], \quad (42)$$

from which the approximate SDE

$$dx = \frac{x}{1+\beta\tau x}[\alpha - \beta(1+\tau\sigma^2)x]dt + \sigma x\, dW \quad (43)$$

is obtained.

Similarly to what is observed for the delayed linear Langevin equation, $f_a(x_o)$ and $\bar{f}^s(x_o|\phi)$ are different. The drift $f_a(x_o)$ has three fixed points: $x_1=0$, $x_2=\alpha/\beta$, and $x_3 = -1/\beta\tau$. However, the origin is repelling as in the original

SDDE. Thus $x_3$ is never approached. Linearizing $f_a(x_o)$ around $x_2$ leads to the eigenvalue $-\alpha(1+\alpha\tau)$. On the other hand, $\bar{f}^s(x_o|\phi)$ has only two fixed points, $x_1=0$ (which is unstable) and $x_2=\alpha/[\beta(1+\tau\sigma^2)]$. Linearizing $\bar{f}^s(x_o|\phi)$ around the second fixed point leads to the eigenvalue $-\alpha(1-\alpha\tau)$, which becomes less negative as $\tau$ increases. As for the delayed linear Langevin equation, the effective scaling of the noise induced by the delay in the diffusion term of Eq. (37) more than offsets the drift of the largest eigenvalue towards more negative values.

As mentioned in Sec. III, a systematic quadratic order expansion can lead to quite dramatic changes in the conditional average drift. Indeed, carrying such an expansion on Eq. (42) leads to

$$\bar{f}^s(x_o|\phi) = x_o[\alpha - \beta x_o + \tau\beta x_o(\beta x_o - \alpha - \sigma^2)], \quad (44)$$

for which $\lim_{x\to\infty} \bar{f}^s(x|\phi) = +\infty$, in contrast with $-\infty$ for Eq. (42). Since $\lim_{x_o,x_\tau\to\infty} f(x_o,x_\tau) = -\infty$, the original expression of $\bar{f}^s(x_o|\phi)$ is clearly preferable. Using Eq. (44) as the conditional average drift would require that a boundary condition be externally imposed in order to prevent the system from diverging. This example illustrates that one must be careful when carrying out expansions on results which follow from the integration of expanded differential equations. After the original expansion has been carried out, it is often wise, whenever possible, to postpone any additional approximation until the end of the calculation. This allows a more complete analysis of the implications of such approximations.

### 3. Numerical simulations

For the simulations, Eq. (36) is interpreted using Stratonovich calculus and is transformed into an equivalent Ito SDDE, as shown in the Appendix, thus leading to Eq. (A7). All the analytical expressions used in the figures are therefore those derived using Stratonovich calculus and presented in the Appendix. This calculus is used in order to simplify comparisons with future studies on delay differential equations subjected to colored noise.

Similarly to what is done for the delayed linear Langevin equation in Sec. IV A 4, $t$ is scaled by $\alpha^{-1}$ and $x$ by $\alpha/\beta$. Furthermore, since the main focus of this paper is to discuss the small delay approximation, and not to completely characterize the logistic SDDE, $\alpha/\beta^2$ is fixed to 1 for the simulations. This being so, Eqs. (A7) and (A8) are recovered with $\alpha=\beta=1$.

As was done for the linear SDDE, the simulations were performed using a fixed step-size stochastic Euler scheme. Again, the integration step size was varied between $10^{-3}$ and $10^{-5}$, and was never larger than one thousandth of the delay. All the results were calculated from 100 realizations, each spanning on the order of $10^7$ integration steps. Here again, the error bars on each point are either smaller than the symbol used in the graph or of similar size.

As seen from Fig. 5, for a delay of 0.1 and a noise variance of 1.0, there is only an 8% difference between the mean of the steady-state probability density for the approximate SDE (A8) and the value obtained numerically from simulating SDDE (A7), and a 20% difference in the case of the
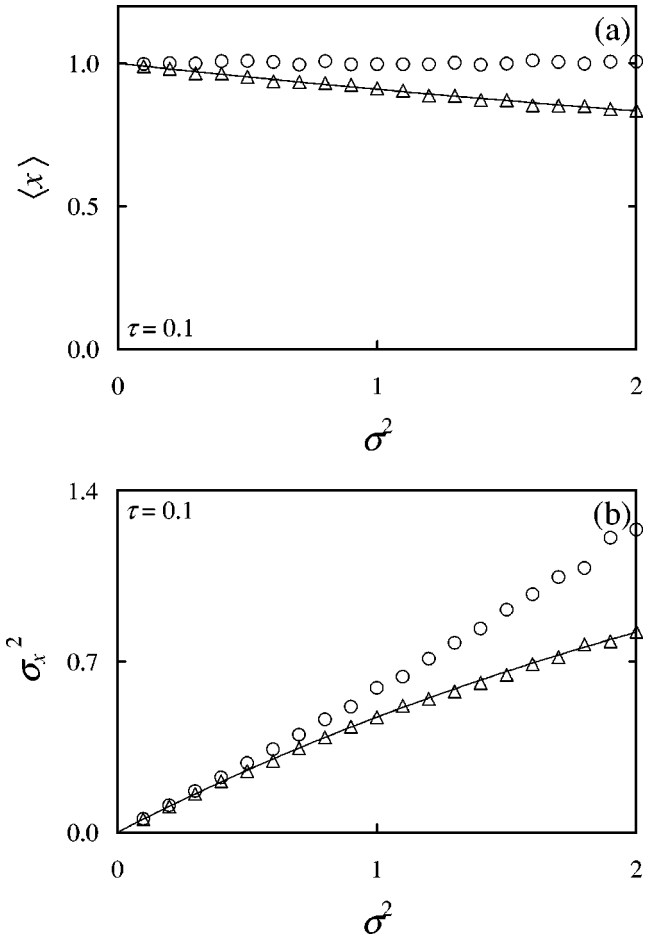


FIG. 5. Mean and variance of the steady-state probability density for the logistic SDDE (A7) and the approximate SDE based on $f_a(x_o)$ and $g_a(x_o)$ [Eq. (A8)] as a function of noise variance. The circles and triangles represent simulation results for, respectively, the logistic SDDE and its approximate SDE. In (a), the line represents the mean as given by Eq. (A10), and in (b) represents the variance as given by Eq. (A11).

variance. Although Fig. 5 indicates that the noise variance can contribute to the degradation of the small delay approximation, Fig. 6 shows that the qualitative agreement between the approximate steady-state probability density and simulation results for the SDDE remains excellent for large values of noise variance. This is true even though a noise-induced transition, as defined by Horsthemke and Lefever [18], has occurred.

As the delay increases, Fig. 7 shows that the approximation is quantitatively good up to about $\tau=0.5$, at which point there is about a 5% difference between the exact value of the mean and its approximate expression, and around 20% difference for the variance. However, the approximation is still qualitatively good up to about $\tau=0.9$ (Fig. 6). As the delay increases up to about 1.4, simulations indicate that a transition occurs in which the slope of the steady-state probability density changes from zero to infinity at the origin (not shown). If the delay is further increased, the probability density diverges at the origin (not shown). As expected, these two transitions are not predicted by the small delay approximation.
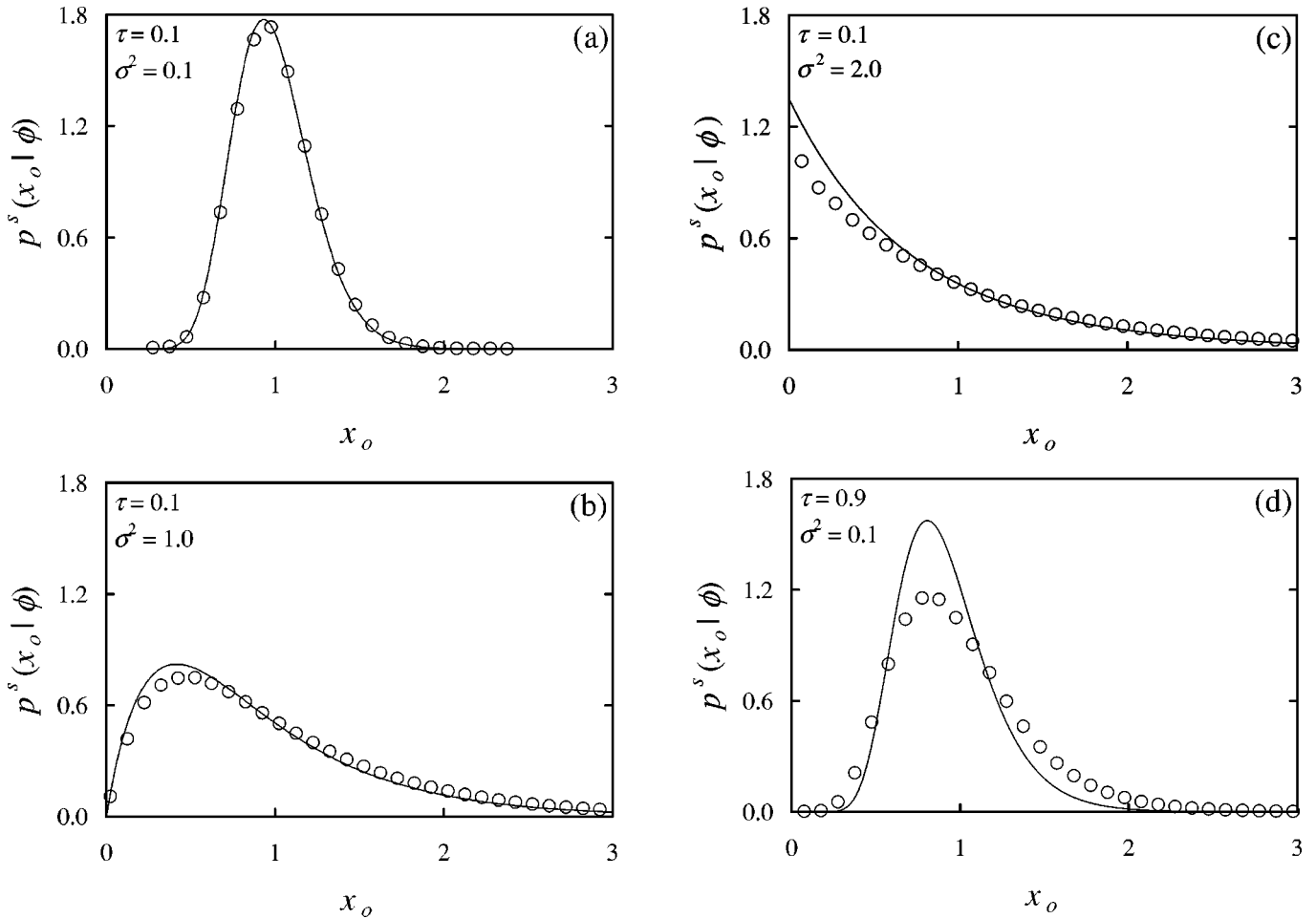
FIG. 6. Probability density for the logistic SDDE (A7) for four combinations of $\tau$ and $\sigma^2$. The circles represent simulation results for the exact SDDE, and the line the approximate probability density given by Eq. (A9).

Figure 8 once again demonstrates that $\bar{f}^s(x_o|\phi)$ approximates the SDDE's CAD much better than $f_a(x_o)$, and that it should therefore lead to dynamical properties which are much closer to those of the original SDDE.

Overall, for this nonlinear SDDE, the small delay approximation is seen to be very good for small delays, even as the noise variance increases. Furthermore, it remains reasonably good for delays which are far from being negligible ($\tau \approx 0.5$).

## V. DISCUSSION

As seen in Sec. II, the usual approach to obtain a Fokker-Planck equation fails when applied to Eq. (1), since $\bar{f}(x_o,t|\phi)$ requires prior knowledge of the conditional probability density $p(x_\tau,t-\tau|x_o,t;\phi)$. Approximation schemes are therefore required in order to obtain a FPE for problems involving SDDE's.

This paper basically presents a simple analytical recipe for the transformation of a large class of SDDE's with a short delay into approximate SDE's, opening the door to all the analytical tools which have been devised for the latter. Since the linearization of a first-order SDE around a fixed point can only have a real eigenvalue, our approach may yield close agreement with numerical simulations of a SDDE only in regimes for which possible oscillatory modes are

strongly damped. Otherwise, however, our method makes possible studies of the effect of shorts delays in many stochastic systems where they have been previously neglected.

The simple quadratic order Taylor expansion presented in Sec. III leads, for short delays, to steady-state probability densities which are in close agreement with numerical results. One detail must however be stressed: even though the delay appears only in the drift term of the initial SDDE, it appears in both the drift and the diffusion terms of the approximate SDE derived using the Taylor expansion. This fact implies that the noise term must be included before the expansion. Otherwise, the resulting approximate system would be flawed. In fact, for the linear SDDE, it would lead to a decreasing variance as the delay increases, which is the opposite of what is observed for the SDDE. This is also the origin of the main difference between the SDE obtained directly from the Taylor expansion and the one based on the CAD. Whereas the deterministic eigenvalue from the drift term of the former behaves in the same way as the corresponding deterministic eigenvalue of the SDDE as the delay is varied, this is not true for the latter. Because the approximate SDE based on the CAD has the same diffusion term as the original SDDE, its drift term accounts for the influence of the delay on both the drift and diffusion terms of the SDE derived using the Taylor expansion. Indeed, as illustrated by the two examples presented in Sec. IV, the deterministic ei-
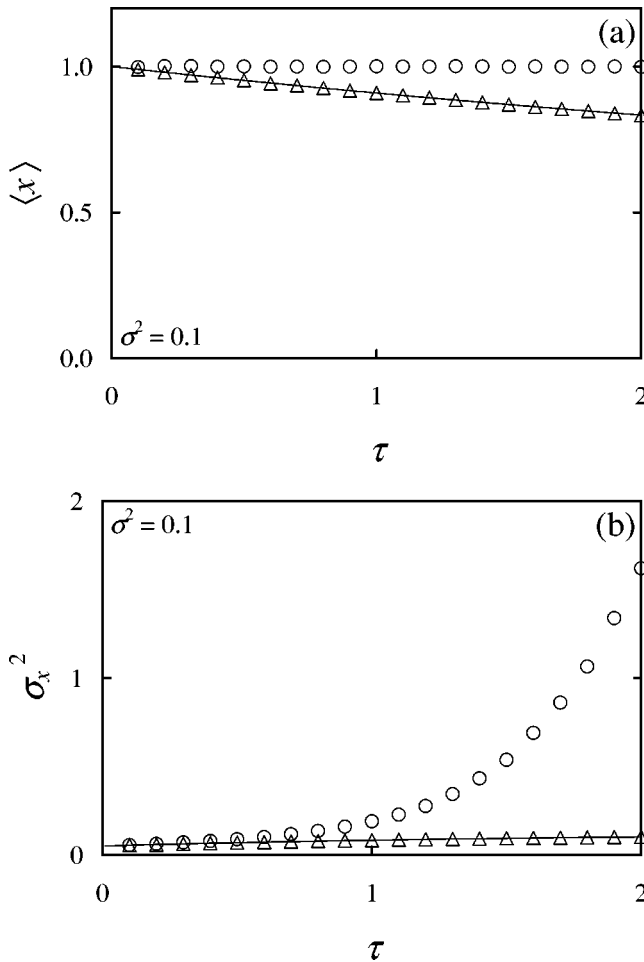
FIG. 7. Mean (a) and variance (b) of the steady-state probability density for the logistic SDDE (A7), as in Fig. 5, but as a function of delay.

genvalue of the SDE based on the CAD intuitively agrees with the behavior of the probability density as the delay is varied, i.e., the variance of the steady-state probability density increases as the real part of the eigenvalue becomes less negative. Therefore, even though both approximate SDE's lead to the same approximate steady-state probability density for the SDDE, their dynamical behaviors are different. They therefore represent two complementary tools when studying the small delay regime of a SDDE.

The approach presented in this paper does not depend on the color of the noise. In fact, it can be used with any type of noise. It can also be easily generalized to a system with multiple delays. Futhermore, another interesting extension of the theory presented here is to consider noisy delays, that is, systems on which noise is applied on the delay itself and not only on the dynamical quantities.

In Eq. (1), the delayed variable $x(t-\tau)$ does not appear in the multiplicative term. The reason for this is that it yields nonlinear noise in the approximate SDE resulting from the Taylor expansion, even for quadratic order expansions in the delay. Much caution is required in order to properly interpret nonlinear noise and take its white noise limit. A rigorous analysis of the effect of delayed multiplicative terms is forthcoming.

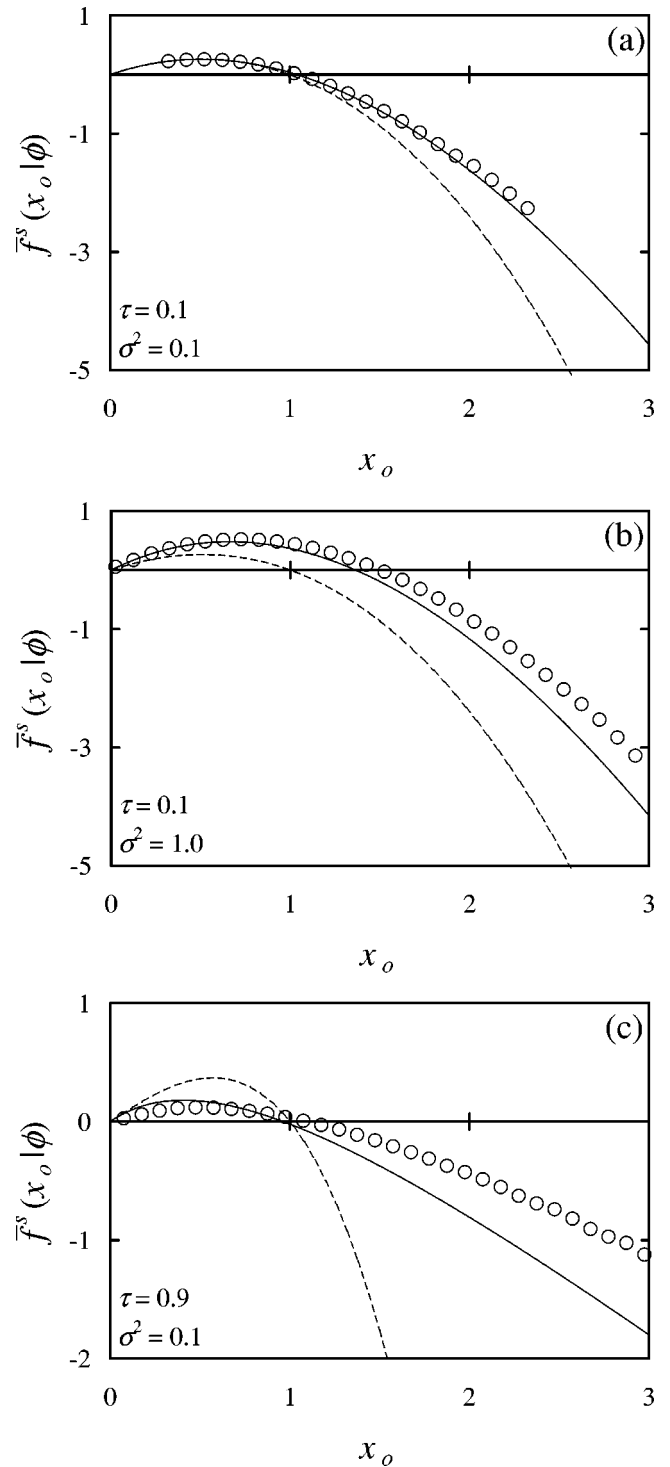This research has concentrated on the small delay ap-



FIG. 8. Steady-state CAD of the logistic SDDE (A7) for three combinations of $\tau$ and $\sigma^2$. The circles represent simulation results for the exact SDDE. The continuous line is the approximate steady-state CAD of the logistic SDDE as given by Eq. (A12), and the dashed line the drift function $f_a(x_o)$ from Eq. (A8).

proximation as a case where the number of degrees of freedom can be reduced to a manageable amount. The large delay limit, where the system may sometimes be reduced to a map, is another case where such a projection may be possible. Finally, approximate formulations of the SDDE in terms of coupled ODE's could possibly be used to study the intermediate delay regime.

## APPENDIX: STRATONOVICH FORMULAS

In this paper, the theoretical analysis is performed using Ito calculus. Equivalent Stratonovich results are summarized in this appendix.

### 1. Fokker-Planck equation

A Stratonovich SDDE can be transformed into an equivalent Ito SDDE using the transformation

$$f(x_o,x_\tau) \rightarrow f(x_o,x_\tau) + \frac{\sigma^2}{2} g(x_o) \frac{d}{dx_o} g(x_o) \qquad (A1)$$

in analogy with the non-delayed stochastic differential equation case [17]. If Eq. (1) is interpreted using Stratonovich calculus, its equivalent Ito formulation is thus

$$dx(t) = \left[ f(x(t),x(t-\tau)) + \frac{\sigma^2}{2} g(x(t)) \frac{d}{dx_o} g(x(t)) \right] dt + \sigma g(x(t)) dW(t). \qquad (A2)$$

This equation can now be subjected to the same analysis as Eq. (1). This analysis remains valid as long as the transformation (A1) is applied to every definition and result where the drift term $f(x_o,x_\tau)$ appears. In particular, the CAD is now defined as

$$\bar{f}(x_o,t|\phi) \equiv \int_a^b dx_\tau \left[ f(x_o,x_\tau) + \frac{\sigma^2}{2} g(x_o) \frac{d}{dx_o} g(x_o) \right] p(x_\tau,t-\tau|x_o,t;\phi). \qquad (A3)$$

Once the CAD is defined using Eq. (A3), the Fokker-Planck equation associated with Eq. (A2) is given by Eq. (10), and the steady-state probability density by Eq. (12). Furthermore, Eq. (13) can still be used to calculate the steady-state limit of the CAD.

### 2. SDDE expansion to $O(\tau^2)$

Using transformation (A1), the approximate drift $f_a(x_o)$ is now defined as

$$f_a(x_o) \equiv \left( f(x_o,x_o) + \frac{\sigma^2}{2} g(x_o) \frac{d}{dx_o} g(x_o) \right) \left( 1 - \tau \frac{\partial}{\partial x_\tau} f(x_o,x_o) \right), \qquad (A4)$$

while $g_a(x_o)$ is still given by Eq. (15b). Equation (17), which yields the steady-state probability density, is expressed in terms of $f_a(x_o)$ and $g_a(x_o)$, and therefore remains unchanged. On the other hand, the CAD [Eq. (18)] is now approximated by

$$\bar{f}^s(x_o|\phi) = \frac{f(x_o,x_o) + \frac{\sigma^2}{2} g(x_o) \frac{d}{dx_o} g(x_o) + \tau\sigma^2 g^2(x_o) \left[ \frac{d}{dy} \frac{\partial}{\partial x_\tau} f(y,y) \right]_{y=x_o}}{1 - \tau \frac{\partial}{\partial x_\tau} f(x_o,x_o)}. \qquad (A5)$$

### 3. Applications

#### a. Delayed linear Langevin equation

Since in this system the noise is additive, transformation (A1) is trivial, and both Ito and Stratonovich calculus lead to the same results.

#### b. Delayed logistic equation

For this system, transformation (A1) reduces to

$$\alpha \rightarrow \alpha + \frac{\sigma^2}{2}, \qquad (A6)$$

which must be applied to every equation in Sec. IV B.

In particular, if Eq. (36) is interpreted using Stratonovich calculus, the equivalent Ito SDDE is

$$dx(t) = \left[ \alpha + \frac{\sigma^2}{2} - \beta x(t-\tau) \right] x(t) dt + \sigma x(t) dW(t). \qquad (A7)$$

The associated approximate SDE then becomes

$$dx = (1+\beta\tau x) \left( \alpha + \frac{\sigma^2}{2} - \beta x \right) x \, dt + (1+\beta\tau x) x \, dW, \qquad (A8)$$

and the approximate steady-state probability density is

$$p_a^s(x_o|\phi_o) = \frac{N_a x^{2\alpha/\sigma^2 - 1}}{(1+\beta\tau x)^{2(\tau^{-1}+\alpha)/\sigma^2+3}}. \qquad (A9)$$

The mean of this steady-state probability density is given by

$$\langle x \rangle = \frac{\alpha}{\beta(1+\tau\sigma^2)}, \tag{A10}$$

and its variance by

$$\sigma_x^2 = \frac{\sigma^2\alpha[1+\tau(\alpha+\sigma^2)]}{2\beta^2(1+\tau\sigma^2)^2\left(1+\tau\dfrac{\sigma^2}{2}\right)}. \tag{A11}$$

Contrary to what is observed when calculating the moments for the Ito case, $\sigma^2$ is not restricted to values smaller than $2\alpha$. Finally, the steady-state CAD becomes

$$\bar{f}^s(x_o|\phi) = \frac{x_o}{1+\beta\tau x_o}\left[\alpha + \frac{\sigma^2}{2} - \beta(1+\tau\sigma^2)x_o\right]. \tag{A12}$$

---

[1] K. Ikeda, H. Daido, and O. Akimoto, Phys. Rev. Lett. **45**, 709 (1980).

[2] F. A. Hopf, D. L. Kaplan, H. M. Gibbs, and R. L. Shoemaker, Phys. Rev. A **25**, 2172 (1982).

[3] P. Nardone, P. Mandel, and R. Kapral, Phys. Rev. A **33**, 2465 (1986).

[4] K. Ikeda and K. Matsumoto, Physica D **29**, 223 (1987).

[5] P. J. Wangersky and W. J. Cunningham, Ecology **38**, 136 (1957).

[6] M. C. Mackey and L. Glass, Science **197**, 287 (1977).

[7] A. Beuter, J. Bélair, and C. Labrie, Bull. Math. Biol. **55**, 525 (1993).

[8] J. G. Milton, A. Longtin, A. Beuter, M. C. Mackey, and L. Glass, J. Theor. Biol. **138**, 129 (1989).

[9] C. M. Marcus and R. M. Westervelt, Phys. Rev. A **39**, 347 (1989).

[10] M. C. Mackey, J. Econ. Theory **48**, 497 (1989).

[11] M. R. Roussel, J. Phys. Chem. **100**, 8323 (1996).

[12] A. Longtin, J. G. Milton, J. E. Bos, and M. C. Mackey, Phys. Rev. A **41**, 6992 (1990).

[13] K. Vasilakos and A. Beuter, J. Theor. Biol. **165**, 389 (1993).

[14] Y. Chen, M. Ding, and J. A. S. Kelso, Phys. Rev. Lett. **79**, 4501 (1997).

[15] J. García-Ojalvo and R. Roy, Phys. Lett. A **224**, 51 (1996).

[16] R. Kapral, E. Celarier, P. Mandel, and P. Nardone, in *Optical Chaos*, Vol. 667 of *Proceedings SPIE (International Society for Optical Engineering)* (SPIE, Bellingham, WA, 1986), pp. 175–182.

[17] C. W. Gardiner, *Handbook of Stochastic Methods for Physics, Chemistry and the Natural Sciences*, Springer Series in Synergetics, 2nd ed. (Springer-Verlag, New York, 1990), Vol. 13.

[18] W. Horsthemke and R. Lefever, *Noise-Induced Transitions. Theory and Applications in Physics, Chemistry, and Biology*, Springer Series in Synergetics Vol. 15 (Springer-Verlag, New York, 1984).

[19] A. Longtin, Phys. Rev. A **44**, 4801 (1991).

[20] X. Mao, SIAM (Soc. Ind. Appl. Math.) J. Math. Anal. **28**, 389 (1997).

[21] D. R. Bell and S.-E. A. Mohammed, Ann. Prob. **23**, 1875 (1995).

[22] U. Küchler and B. Mensch, Stoch. Stoch. Rep. **40**, 23 (1992).

[23] M. C. Mackey and I. G. Nechaeva, Phys. Rev. E **52**, 3366 (1995).

[24] T. Ohira, Sony Computer Science Laboratory Technical Report No. SCSL-TR-96-010, 1997 (upublished).

[25] T. Ohira, in *Proceedings of the 3rd Workshop on Orders and Structures in Complex Systems* (International Institute for Advanced Studies, Kyoto, 1996), pp. 74–78.

[26] J. Losson and M. C. Mackey, Phys. Rev. E **52**, 115 (1995).

[27] J. M. Cushing, *Integrodifferential Equations and Delay Models in Population Dynamics*, Lecture Notes in Biomathematics Vol. 20 (Springer-Verlag, New York, 1977).

[28] T. L. Saaty, *Modern Nonlinear Equations* (Dover, New York, 1981).

[29] E. M. Wright, J. Reine Angew. Math. **194**, 66 (1955).

[30] A. Papoulis, *Probability, Random Variables, and Stochastic Processes*, 3rd ed. (McGraw-Hill, New York, 1991).

[31] J. Hunter and J. G. Milton (private communication).